Received: 2 February 2024 | Revised: 6 September 2024 | Accepted: 18 September 2024

IET Renewable Power Generation

DOI: 10.1049/rpg2.13141

The Institution of Engineering and Technology WILEY

ORIGINAL RESEARCH

Integration of a solid oxide electrolysis system with solar thermal and electrical energy: A testing campaign for operation and control strategy definition

Elena Crespi | **Francesca Panaccione** | **Davide Ragaglia** | **Matteo Testi**

Fondazione Bruno Kessler, Sustainable Energy Center, Povo, Italy

Correspondence
Elena Crespi, Fondazione Bruno Kessler, Sustainable Energy Center, Povo, Italy.
Email: ecrespi@fbk.eu

Funding information
Fuel Cells and Hydrogen Joint Undertaking, Grant/Award Number: 101007194

Abstract

The EU project PROMETEO has the scope of testing a 25 kW solid oxide electrolysis system integrated with a concentrated solar power plant via thermal energy storage in a relevant environment. Given the plant layout and the hydrogen demand characteristics, this work aims to identify how to operate the system effectively when renewable electricity is unavailable and how to modulate the load during hydrogen generation, thus defining the system's operation modes and control strategy. A 5 kW_e stack has been tested at the FBK facility. The hot standby tests show that feeding a reducing gas at the negative electrode and air at the positive electrode, without polarizing the stack, effectively keeps the stack hot at 750°C and prevents degradation. Conversely, the electric protection approach leads to significant stack degradation (15% voltage drop in 200 h for one cluster). Regarding modulation of hydrogen generation, with low steam flowrates, the stack current and the flow rate of produced hydrogen mainly depend on the steam flow rate, while it is not affected by the stack temperature; conversely, with high steam flowrates, the current depends only on the stack temperature (from 25 A at 670°C to 65 A at 760°C). Based on the results, two hot standby modes and two load control strategies to be implemented and tested in the PROMETEO prototype are proposed.

1 | INTRODUCTION

1.1 | Motivation and background

The growing concern about the negative environmental impact of using fossil fuels for energy production and the growing energy demand have led to an increasing use of alternative renewable energy sources, namely wind power plants and photovoltaic (PV) systems. Since these technologies are unprogrammable and non-predictable, their increasing penetration into the power grid hinders grid stability, thus raising the need for regulation reserve and storage systems. In this framework, an energy vector such as hydrogen can fundamentally store renewable electricity. The production of renewable hydrogen through the electrolysis of water using renewable electricity, without any pollutant emission, can also link the electrical grid to the gas and thermal grids, allowing the decarbonization of the sectors that cannot be electrified [1]. Among them are the so-called 'hard-to-abate sectors', including energy-intensive industries and industries already using hydrogen of fossil origin as feedstock (e.g. for ammonia and fertilizer production). Indeed, more than 90% of hydrogen used today is produced by steam reforming of methane.

Water electrolysis systems can store renewable electricity by producing hydrogen without any emission of greenhouse gasses. Different electrolysis technologies have been studied. They are mainly divided between low-temperature electrolysers, working with liquid water, and high-temperature electrolysers, working with steam. Among these technologies, the highest technology readiness levels (TRL) are reached by the alkaline and the proton exchange membrane (PEM) technologies, both with TRL 9 [2]. These are low-temperature systems, mainly characterized by fast starting, wide operating range and rapid load variations. However, high-temperature electrolysis systems are emerging, mainly represented by the solid oxide electrolysis (SOE) technology, which shows some advantages compared

to the commercial low-temperature technologies, although the lower TRL (TRL = 7).

The integration of SOE systems with solar and wind generators looks promising to increase the penetration of RES in the power grid. For instance, [3] shows the role of a SOE system in tackling the challenge of dispatching renewable electricity in a microgrid (namely the University of California, Irvine campus microgrid), allowing to effectively increase the penetration of renewable electricity from PV and wind by decoupling electricity production and energy consumption through the production of hydrogen. Indeed, the important role that storage solutions have in facing the unpredictability and variability of RES has been widely investigated, also underlining the importance of an optimize planning of RES and storage distribution. For instance, [4] shows that energy storage integration is an effective and feasible way to improve the power output performance of renewable distributed generators and highlights the importance of novel optimization methods to plan their distribution effectively, reaching better voltage stability, lower line losses and higher investment benefits.

Compared to other electrolysis technologies, SOE systems, working at about 700°C, have the potential to reach a higher electrical efficiency [5–9] and can also be operated in fuel cell (FC) mode to co-generate electricity and heat from hydrogen (i.e. they are reversible systems) [10]. On the other hand, the high temperature and the polarization of the electrodes promote degradation mechanisms, affecting the mechanical stability of these systems in long-term operation and requiring more expensive materials [11]. Additionally, to enable these systems to work at high temperatures, thermal power has to be supplied in addition to the electrical power. Heat is required to evaporate the water, which has to enter the stack as steam, to compensate for the thermal losses and to keep the system at the defined operating temperature [12]. Thus, besides improving the electrolysis stack components and assembly to enhance performance and limit degradation, research is focused on improving heat management at the system level [13]. An optimized thermal integration, allowing the recovery of as much heat as possible from the exhaust gas to preheat the inlet flows, is fundamental to minimize the need for external heat, whose contribution is not negligible. External heat sources are therefore required [14]. Thus, supplying the system with low-cost heat results necessary to exploit the advantage derived by the high-temperature operation, minimizing the electricity consumption and maximizing the electrical efficiency. Possible solutions include the utilization of waste heat [15] or renewable heat sources, such as geothermal energy [16, 17] or solar heat [18]. With reversible solid oxide systems, working both in FC and electrolysis mode, heat integration is possible. For instance, [19] have shown that the use of a thermal energy storage, consisting of a phase change material, allows to exploit the heat produced by the exothermic reactions in FC mode to self-sustain the endothermic reactions in electrolysis mode and to heat-up the inlet streams.

Besides thermal management, another challenge is the integration of SOE stack with renewable power sources, whose electricity generation is unpredictably fluctuating. The feasibility of coupling SOE systems with wind generators has been explored in [20] where, in a 2014-hours test alternating steady state and dynamic operation, no signs of additional degradation during dynamic operation were found. The possibility to operate SOE systems with on-off intermittent conditions without strongly impacting the degradation rate has been proved in [21], where the effects of intermittent operation on SOE cells performance have been investigated with 600 h tests both in steady-state and in transient conditions (avoiding thermal variation and maintaining a reducing atmosphere at the hydrogen electrode). However, this study highlights the need to further study the transient operation in practical operating conditions, such as startup, shutdown, power fluctuation, and thermal cycling. The impact that the thermal stress caused by frequent deviation from the optimal operating condition has on the cell performance has been studied in [13], where a model has been developed and used to show that the distribution of thermal stress is affected by the temperature and flow rate of the inlet gas.

1.2 | PROMETEO Project overview and contribution of the study

In this framework, the PROMETEO project [22] is a European Horizon 2020 project aimed at designing, building, and testing an electrolysis system based on SOE cells and fully integrated with a renewable power source (namely, a photovoltaic field and/or wind turbines) and a concentrated solar power (CSP) unit. The innovative system will produce green hydrogen using renewable power and heat from the sun. Alternatively, withdrawing electric power from the grid when the electricity price is low is also foreseen.

Integrating the SOE system with renewable energy sources is the peculiarity and the main challenge of the PROMETEO project. Indeed, PV, wind, and CSP plants are unpredictable, non-constant and uncontrollable. It follows that thermal energy from the CSP plant may not be available when electricity is low-cost. Thus, the project is aimed at optimizing the SOE system coupling with intermittent sources of electricity (PV, wind, or cheap grid power) and high-temperature solar heat (from the CSP system) through the integration of a thermal energy storage (TES) and, possibly, of a battery. The system design considers end-users needs, the technology readiness of system components, sustainability aspects, regulatory and safety issues, and the need for a future scale-up to the relevant industrial size. Thanks to an optimized design and control strategy, the proposed integrated system will increase the efficiency, flexibility, and reliability of SOE electrolysers while minimizing hydrogen production costs.

A preliminary design of the PROMETEO pilot plant has already been defined (a simplified system layout is described in [23]). The fully equipped prototype will install a 25 kW_e SOE stack (about 15 kg/day of nominal hydrogen production) and will be tested and validated in real contexts, reaching TRL 5. Three case studies have been identified to be tested within the project. They are power to gas (P2G) applications related

to hydrogen production for uses which differ from electricity generation. The three identified case studies, differing for conditions and requirements both upstream and downstream of the electrolysis system, are:

(i) Production of ammonia with both grid- and PV-generated electricity. In this case, constant hydrogen generation is required to produce ammonia. Thus, the electrolyser has to work constantly at full load. Furthermore, a constant supply of electricity is guaranteed thanks to the connection with the power grid.
(ii) Production of hydrogen for injection into the gas grid with both grid- and PV-generated electricity. In this case, hydrogen is injected into the natural gas grid to a maximum hydrogen percentage of 2% in volume. As in case i), it is possible for the electrolyser to work at full load since a constant supply of electricity is provided by a power grid connection.
(iii) Production of hydrogen for injection into the gas grid with PV-generated electricity only. As in the previous case, hydrogen is injected into the natural gas grid to a maximum hydrogen percentage of 2% in volume. However, in this case, a constant operation at full load is not possible, and partial load operation is required to generate H_2 when the available power is reduced. Additionally, a hot standby mode and a night mode are required to keep the system hot when electricity is not available, thus allowing to rapidly start the system and generate hydrogen when the electricity is available again.

Within the PROMETEO Project, this work aims to define the operation modes and the control strategy for the pilot SOE system, considering the characteristics of the end-users' hydrogen demand and the availability of renewable heat and electricity. This is required for the effective management of the plant, both when renewable and/or low-cost electricity is available and hydrogen generation must be modulated and controlled to satisfy the demand, and when electricity is not available, hydrogen cannot be produced, and the system performance must be preserved.

In this framework, testing the SOE stack is of key importance to understand the impact of the operating conditions on the stack performances over time, thus developing a safe and reliable control of the system improving the performance while automatizing the system operation.

1.3 | Literature review

Although developing a suitable control strategy is essential for guaranteeing a safe and efficient system operation, few studies exist on this topic. Some include experimental testing of SOE stacks, while others perform system simulations.

In the experimental studies, Udagawa et al. [24] tested an intermediate temperature SOE stack for hydrogen production. They analysed the correlation between the air flow rate and stack temperature, finding that a higher air flow rate guarantees a more homogeneous stack temperature, providing enhanced cooling for the stack during exothermic operation and enhanced heating during endothermic operation. At the same time, a slight dependence of the stack temperature on the air flow rate is identified at thermoneutral conditions, indicating that, in this case, controlling the temperature through a variation of the airflow rate should be avoided. Fragiacomo et al. [25, 26] performed an experimental campaign on a solid oxide stack in electrolysis and Fuel Cell operation mode. As regards the electrolysis operation, the experimental activity consisted of ten tests, where different gas mixtures (binary of H_2-steam mixtures in the first nine tests, ternary H_2-steam-CO_2 mixture in the last one) and air at different temperatures (650, 700, and 750°C) were fed to the stack. They show that the H_2 production of the SOE stack increases with increasing air temperature, and the highest H_2 production is obtained by feeding the stack with the highest steam content in the mixture (90%). Barelli et al. [27] analysed the role of the airflow rate when used as a sweep gas in the oxygen electrode of an SOE system. This experimental activity shows that the stack's performance is not significantly affected by the airflow rate (voltage variation below 2% with an airflow rate variation from the nominal value down to 9%). Peters et al. [28] analysed and experimentally tested a reversible solid oxide stack (i.e. working in both FC and electrolysis mode), conducting a parametric analysis to show how the efficiency varies as function of the fuel utilization and the recirculation fraction. For the electrolysis mode, the efficiency value increases with increasing steam utilization and stack power.

Some authors rely on system modelling and simulations to study SOE system operation with time-varying currents generated by intermittent renewable energy sources. For instance, Lu et al. [29] developed a control-oriented SOE dynamic model (validated with data from the literature), which implements adaptive feedback control to stabilize the temperature of the SOE stack. The control acts on the air flow rate when operating at a low current density, below the thermoneutral value, and on the fuel flow rate when operating at a higher current density. Cai et al. [30] used a model of an SOE system (including only the stack and the compressor) coupled with intermittent renewable energy sources to identify the optimal operation strategy. In particular, the study aims to maximize hydrogen production, minimizing SOE energy consumption and minimizing the compressor energy consumption, while ensuring the stack temperature control with constraints on the overall temperature difference across the cell and the temperature gradient. Botta et al. [31] developed a dynamic model of the SOE system to investigate the dynamic behaviour and to select the optimal control strategy. The study shows that temperature and reactant utilization control is crucial during transient operation to avoid fuel starvation and to minimize temperature variation, thus preventing thermo-mechanical stress to the main components.

Overall, experimental studies investigate the SOE stack behaviour when producing hydrogen in different operating conditions, mainly analysing the effects of different air flow rates, air temperatures, and steam compositions. Conversely, models are used to study the system control, mainly focusing on stack temperature control during hydrogen production.

However, the existing studies do not give any information related to the source of heat for the stack or on how to operate the system when renewable electricity is unavailable (e.g. at night), during the warm-up phase, or transient operation.

1.4 | Novelty of the study and paper organization

Testing and characterizing a SOE stack during full load, partial load and hot-standby operation is required to identify how to operate the system effectively when renewable electricity is unavailable and how to modulate the load during hydrogen generation, thus defining the system's operation modes and control strategy.

This work includes an innovative analysis of a 5 kW SOE stack, which is tested at nominal full load operation, partial load, and hot standby mode. It describes an experimental campaign performed at Fondazione Bruno Kessler (FBK) facilities to support the definition of the system operating conditions in each operating mode and the SOE system's management and control strategy. The test activity is divided into two campaigns, studying the stack behaviour in the standby mode (without electricity supply) and in operation mode (with the electricity supply).

The paper is organized as follow. Chapter 2 introduces materials and method, describing the test bench and the stack characteristics (Section 2.1), the test campaign for analysing the stack hot standby (Section 2.2) and the test campaign for defining the hydrogen generation control (Section 2.3). Chapter 3 presents and discuss the results of the stack hot standby analysis testing campaign (Section 3.1) and of the hydrogen generation control definition testing campaign (Section 3.2). Finally, Chapter 4 draws the conclusion, proposing possible management and control solutions to be implemented and tested in the PROMETEO pilot plant.

2 | MATERIALS AND METHOD

The analysis of the case studies identified in the PROMETEO project has shown the need to operate the SOE system at full and partial loads and to implement a standby mode. Indeed, not all applications require constant hydrogen production (e.g. applications ii) and iii) identified in Section 1.1 allow intermittent hydrogen generation). Additionally, a continuous electricity supply is not always possible (as in case iii)). Therefore, there is a need to operate the system at different loads, to follow the electricity availability and the hydrogen demand, and to identify a hot standby mode for the system when hydrogen is not produced.

The core of the work here developed aims to test an SOE stack to understand how it behaves when operated with different operating conditions, such as different electric loads, stack temperature, steam flow rate, and hydrogen concentration in the steam at the cathode inlet. This is essential to identify an effective management and control strategy for the system.

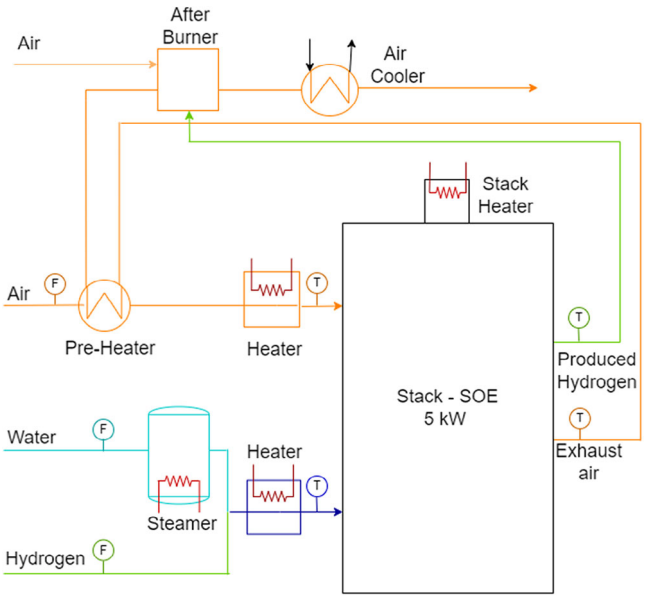

FIGURE 1 Process flow diagram of 5-kW SOE test bench at FBK facility.

Two experimental campaigns have been carried out at the FBK facility on a test bench to test SOE stacks up to 8 kW, testing a 5 kW SOE stack with cells equal to those used in the PROMETEO pilot plant (described in Section 2.1). The main goal of the first experimental campaign (Section 2.2) is to identify the optimal conditions for the system's hot standby mode when hydrogen cannot be produced because of the unavailability of renewable or low-cost electricity (e.g. during the night, when renewable electricity from the sun is not available), but it is necessary to keep the stack warm and to preserve its health. The main goal of the second experimental campaign (Section 2.3) is to determine which parameters mainly affect hydrogen generation, identifying the optimal control strategy to partialize the stack load, as required with low availability of renewable electricity.

2.1 | Test bench and SOE stack characteristics

The experimental activities have been performed on the test bench TB2500, which was developed by EBZ gmbh [32]. The test bench hosted in the FBK H2 facility, designed for experimental testing of solid oxide fuel cell stacks, has been modified to work with SOE stacks by accommodating a dedicated power unit, adding a fuel inlet line (to mix hydrogen with steam, thus guaranteeing a reducing atmosphere in the negative side of cells) and upgrading the software to allow the implementation of the testing protocols (to test the stack with a fully automatic procedure).

The main components of the test bench and the main flowmeters (F) and thermocouples (T) are shown in the flow diagram in Figure 1. The test rig includes a steamer, three electric heaters, two heat exchangers, and a burner. Water is evaporated in a steamer, mixed with hydrogen to create a

TABLE 1 Test bench operating condition ranges.

Parameter [unit]	Range of values
Water flow rate [g/h]	200–2200
Steam production [g/h]	0–2000
Steam temperature [°C]	150–500
Hydrogen flow rate [NL/min]	0–44
Air flow rate [NL/min]	0–400
Anode temperature [°C]	0–800
Cathode temperature [°C]	0–800
Voltage (power unit) [V]	0–200
Current (power unit) [A]	0–140

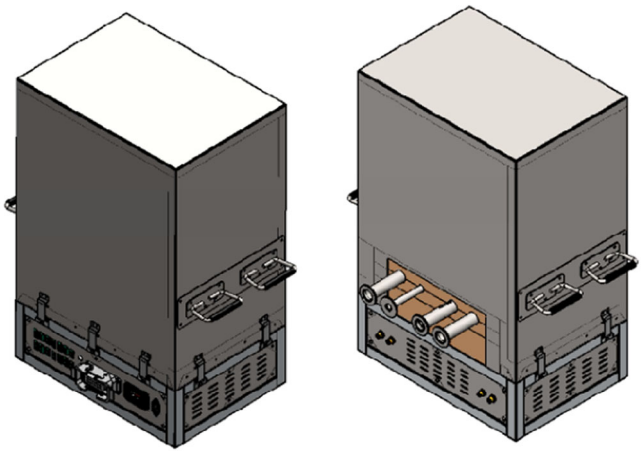

FIGURE 2 SOE stack box, SolydEra S.p.A., Pergine, Italy [33].

reducing environment, heated to the desired temperature in an electric heater and fed to the stack cathode. Air passes through two subsequent components to be heated before entering the stack anode. The air is firstly preheated in a recuperative heat exchanger, recovering heat from the exhaust air, to minimize electricity consumption. Then, the air temperature is precisely controlled with an electric heater. Indeed, a precise control is required because the air temperature is the main parameter affecting the stack temperature. An additional electric heater is installed on the stack, allowing it to operate with a more uniform temperature and accelerate its warm-up. On the exhaust line, the produced hydrogen and the exhaust air are burned in a dedicated after-burner, with additional air. Then, a heat exchanger cools the exhausts before venting. Finally, a power unit supplies the required electric power to the stack.

Table 1 reports the ranges of values that the main system parameters (flow rates, temperature etc.) can assume according to the technical characteristics of the system components. The steamer capacity limits the steam flow rate to 2 kg/h (a higher flow rate would impact steam production stability). The maximum temperature reached by the electric heaters (for air, hydrogen, and stack) is 800°C. Excellent thermal insulation of the air pipes minimizes the thermal losses, and air at the stack inlet can reach a maximum temperature as high as 780°C. Conversely, more significant thermal losses are present in the steam pipes; thus, the maximum temperature of the steam at the stack inlet is 745°C. The power unit (producer code EA-PSI 9200 140) has a peak power equal to 10 kW and a wide span of current (0–140 A) and voltage (0–200 V).

The G8-80 stack (Solydera S.p.A., Pergine, Italy [33]), schematized in Figure 2, is tested. The stack includes 70 single repeated units (SRU) of electrode-supported SOE cells with an active area of 80 cm^2, encapsulated in a stackbox with improved thermal insulation layers and guaranteeing the correct air and fuel connections. The cells are organized into 8 clusters (7 with 9 cells and 1 with 7 cells). The stack works at ambient pressure, and the nominal temperature is between 680 and 780°C.

Different operation modes have been identified for the SOE system to allow its correct operation in the selected case studies (see Section 1.1), satisfying the hydrogen demand while dealing with limited renewable energy availability. Full-load and partial-load modes are identified to guarantee hydrogen production at different rates, either in low hydrogen demand or electricity availability. A hot standby mode is also required to keep the system warm when electricity for H2 production is unavailable.

2.2 | Test campaign for analysing stack hot standby

The first experimental campaign aims to define how to operate the system in the hot-standby mode to keep the system warm when hydrogen is not produced, allowing a fast transition into partial- or full-load modes when required and preserving the stack health. Indeed, to operate synergically with solar electricity, the stack temperature must be kept constant in case of clouds, interrupting the solar irradiation for a limited time (e.g. few minutes), and during the night (few hours). Repetitive cool-down and warm-up of the system are not feasible due to the long time required (many hours) and to the thermal stress induced in the stack components, which is the primary source of degradation of the stack itself.

Therefore, identifying an effective hot-standby mode is of primary importance in preserving the stack performance, mainly preventing the oxidation of the nickel negative electrode. Indeed, the stack is maintained at a high temperature (e.g. 750°C), above 590°C, where oxygen mobility and reactivity are appreciable. At the same time, it is possible that air or water are present at the negative electrode. For instance, air can leak from the positive electrode (flushed with air to keep the stack hot) or reach the negative electrode through the pipelines. Thus, to prevent nickel oxidation, the negative electrode voltage should be maintained above the equilibrium potential of Ni re-oxidation (about 0.8 V at 500°C and 0.7 V at 800°C, assuming an oxygen partial pressure of 0.32 atm) [34].

This study identifies three possibilities to keep the stack warm while preventing nickel oxidation when hydrogen is not produced. Two of them are based on chemical protection of the nickel electrode, while the third proposes an electrical method of protection. The three hot standby (HSB) options,

TABLE 2 Gas composition, flow rate and temperate at anode and cathode inlet, and stack polarization for the three hot-standby options.

		HSB Option 1	HSB Option 2	HSB Option 3
Gas at negative electrode inlet	Composition	20% H_2 80% N_2	20% H_2 80% H_2O (steam)	/
	Flow rate	8.75 NL/min	8.75 NL/min	/
	Temperature	750°C	750°C	750°C
Gas at positive electrode inlet	Composition	Air	Air	Air
	Flow rate	220 NL/min	220 NL/min	150 NL/min
	Temperature	750°C	750°C	750°C
Stack polarization		/	/	70–80 V

characterized by different operating conditions for the stack (summarized in Table 2), are tested in three subsequent phases of the experimental campaign. The performances of the stack are evaluated after each phase of the test to assess the state of health of the stack and compare the effectiveness of each standby option.

In the first standby option (HSB Option 1), the negative electrode is flushed with H_2-enriched forming gas (20% H_2 and 80% N_2) and the positive electrode is flushed with air. The stack is not polarized. The scope is to investigate whether the N_2-H_2 mixture can preserve the electrode's active material, ensuring a sufficient reducing environment while keeping the stack warm.

In the second standby option (HSB Option 2), the negative electrode is flushed with H_2-enriched water steam, and the positive electrode is flushed with air. The stack is not polarized. As in the test of HSB Option 1, the scope is to investigate whether the H_2-steam mixture can preserve the electrode active material and keep the stack warm. Since steam has a higher thermal capacity than nitrogen, using steam would contribute to controlling the stack temperature with a lower air flow rate in the positive electrode, thus reducing possible air leakage to the negative electrode.

In the third standby option (HSB Option 3), the electrical protection approach is tested. The stack is polarized to have an average cell voltage of 1 V, which should prevent the oxidation of the nickel in the negative electrode without flushing it with gas. Thus, the negative electrode is not flushed with gas, while the positive electrode is flushed with air, minimizing the air flow rate to decrease the pressure in the line and consequently the air crossover. The proposed method is based on the electrochemical transport of the oxygen and/or water vapour molecules from the negative electrode to the positive electrode via oxygen-ion conducting electrolyte, such as YSZ (yttria-stabilized zirconia), in a sort of electrochemical pumping of oxygen from the negative to the positive electrode. A similar approach has been proposed for solid oxide fuel cells and tested on a laboratory-scale single cell, showing promising results [35]. However, when many electrolysis cells are electrically connected in series to form a stack, the effectiveness of this approach has to be verified. Indeed, in a stack, the electrochemical pumping of oxygen is limited by the cell with the lowest amount of oxygen/water on the negative side, implying that some cells are well protected (high voltage) while others are exposed to oxygen or water (lower voltage) based on the air amount. Therefore, the scope of the test adopting HSB Option 3 is to investigate whether the electrical protection is applicable in the SOE stack.

Before testing the three hot standby options, the performance of the SOE stack is evaluated with a "health check", which consists of operating the stack in FC mode under specific operating conditions. The health check starts by disconnecting the electric power source (no current applied to the stack), flushing the negative electrode with 8.75 NL/min of H_2-N_2 (80%–20%) gas mixture, and setting the heaters at 750°C. When the system reaches thermal equilibrium, current is drawn from the stack (operating it in FC mode). A linear current sweep from 0 to 32 A (0.4 A/cm^2) is performed, recording the stack voltage. Then, the current is kept at the maximum value (32 A) until the voltage is stabilized, and the voltage of each stack cluster is measured. Finally, a linear current sweep from 32 to 0 A is performed, and the electric load is disconnected. Gas flows to the stacks, temperatures are set back to the operational values, and the power unit is connected.

An initial stack health check is performed, and the three HSB options are consequently tested in the test campaign. Each HSB option is tested for 200 h, and then the stack's performance is evaluated with a health check. Health check results are compared to identify the effectiveness of each HSB option in preserving the stack performance. Additionally, the stack temperature during the hot standby periods is analysed to verify the effectiveness of each HSB option in maintaining the stack at the desired temperature.

2.3 | Test campaign for defining the hydrogen generation control strategy

The main goal of the second experimental campaign is to provide the inputs for identifying a strategy to control the stack load. The test campaign is set up to determine which parameters mainly affect hydrogen generation.

Tests are set up to analyze the effects that temperature, steam flow rate and fraction of hydrogen in the steam at the stack inlet (cathode side) have on the stack operation regarding hydrogen production. All tests have been performed directly controlling the stack voltage (voltage-based control), maintained at the thermoneutral value (V_{th} = 90 V, i.e. 1.29 V/cell) while varying

the temperature, steam flow rate and hydrogen flow rate. While operating at a lower voltage (endothermic conditions) would allow higher electric efficiency, operation at the thermoneutral point is here preferred to avoid temperature gradient in the cells, which would increase cell degradation. Keeping the voltage constant at the thermoneutral value allows to facilitate the thermal management, avoiding moving from exothermic to endothermic operation while changing the load.

Another option would be to consider a direct control of the stack current (current-based control). In this way, unlike the voltage-based control, it would be possible to control the flow rate of produced hydrogen precisely (which is proportional to the current), but a very accurate and fast temperature control would be required to control the stack voltage precisely. Inaccurate temperature control would lead to fluctuations of the stack temperature due to the oscillation between endothermic ($V < V_{th}$) and exothermic ($V > V_{th}$) operating modes of the stack, which would degrade the cells. In addition, the voltage-based control adopted here is a fail-safe control that avoids problems in the event of steam unavailability.

The test campaign has been performed in 2 phases:

- Phase 1: the steam flow rate is varied continuously (it is increased from a minimum value of 360 g/h to a maximum value of 1900 g/h, then decreased back to the minimum value). These values have been chosen considering the operating limits of the steamer. The stack is tested for different values of air and steam temperatures at the stack inlet, ranging from 670 to 760°C. The hydrogen volumetric fraction in the overall steam and hydrogen mixture at the cathode inlet equals 10%, the minimum value to ensure a reducing environment.
- Phase 2: the fraction of hydrogen in the overall steam and hydrogen mixture entering the stack cathode is varied from a minimum value equal to 10% to a maximum value equal to 50% of the steam flow rate, while the steam flow rate is kept constant. The test is repeated for different values of air and steam temperatures at the stack inlet, ranging from 670 to 730°C with stepwise changes of 10°C, and different values of the steam flowrate at the stack inlet, ranging from 360 to 1900 g/h, with fixed stepwise changes of 400 g/h.

The airflow rate at the stack inlet is varied to reach the desired value for the air temperature at the stack outlet, which is considered representative of the stack temperature. At the same time, the hydrogen flow rate is varied to reach the desired fraction of hydrogen in the steam entering the stack.

The free parameter, which is measured, is the stack current (I_{stack}). Its value is proportional to the generated hydrogen (m_{H2gen}) and the absorbed electric power (P_{stack}), as for Equations (1) and (2), respectively, where N_{cell} is the number of cells in the stack (70), MM_{H2} is the molecular mass of hydrogen (2 g/mol), and F is the Faraday coefficient (96485.3 C/mol).

$$I_{stack} = \frac{2\,F}{N_{cell} * MM_{H2}} m_{H2gen} \quad (1)$$

$$I_{stack} = \frac{P_{stack}}{V_{th}} \quad (2)$$

Additionally, the water utilization factor (U_{steam}) is computed starting from the water flowrate entering the steamer ($\dot{m}_{water}$) and the stack current (I_{stack}), according to Equation (3), where MM_{H2O} is the molecular mass of water (18 g/mol).

$$U_{steam}\,[\%] = \frac{\frac{N_{cell} * MM_{H2O}}{2\,F} I_{stack}}{\dot{m}_{water}} * 100 \quad (3)$$

The expected results are charts identifying the stack current (and indirectly, the stack power consumption and hydrogen generation) in different operating conditions. These data are the basis for the implementation of the control strategy.

3 | RESULTS AND DISCUSSION

This section presents the results of the two test campaigns concerning hot-standby analysis and hydrogen generation control definition.

3.1 | Stack hot standby analysis

The hot-standby tests described in Section 2.2 have allowed us to analyse the decay of the stack performance when three different hot standby strategies are adopted. Health checks of the stack are performed at the beginning of the test, and after that, the stack is operated for 200 h in each HSB option.

Figure 3 shows the results of the health checks in terms of stack voltage (left chart) and power density (right chart) as a function of the stack current density. Health check curves 2 and 3, measured after stack operation in HSB option 1 and HSB option 2, overlap health check curve 1, measured at the beginning of the test, showing negligible stack degradation during the two hot standby tests. Conversely, a reduction in the stack voltage and power density is observed after operating the stack in HSB Option 3 (health check 4), highlighting a drop in the stack performance, possibly caused by oxidation of the negative electrode.

In addition to the overall stack voltage, the test bench allows the measurement of the voltage of the cell clusters into which the stack is divided. In analysing the measured cluster voltage, it has to be highlighted that cluster 4 consists of 7 cells only, while the other clusters consist of 9 cells. Figure 4 shows the voltage of each cluster measured during the health checks, with a current density equal to 0.4 A/cm^2. The cluster voltage analysis confirms the goodness of HSB option 1 and HSB option 2, after which minor variations in the cluster voltage concerning the beginning of tests are observed. The cluster voltages don't drop significatively during 200 h in HSB option 1 and during 200 h in HSB option 2. Conversely, HSB option 3 guarantees good protection against degradation for all the clusters (clusters' voltage does not drop significatively) but cluster 1, which shows

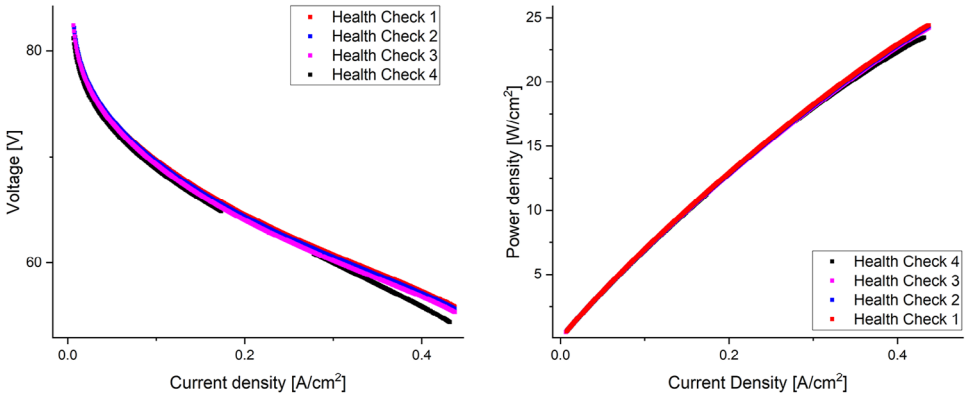

FIGURE 3 Results of stack health checks at the beginning of characterization activity (check 1 – red line), after 200 h in HSB Option 1 (check 2 – blue line), after 200 additional hours in HSB Option 2 (check 3 – magenta line), and after 200 additional hours in HSB Option 3 (check 4 – black line). The left plot shows stack voltage versus current density. The right plot shows power density versus current density.

FIGURE 4 Average cell voltage [V] in each cluster, measured during the stack health checks at the beginning of characterization activity (check 1 – red line), after 200 h in HSB Option 1 (check 2 – blue line), after 200 additional hours in HSB Option 2 (check 3 – magenta line), and after 200 additional hours in HSB Option 3 (check 4 – black line).

a consistent voltage drop close to 15%. The cluster degradation is possibly caused by the oxidation of the negative nickel electrode due to a reverse air flow from the fuel line. Indeed, no check valves are installed in the fuel line, allowing air to flow to the stack, reaching the first cluster. However, the electrode oxidation can be confirmed only with a postmortem test, which was not possible in this study.

Overall, the experimental campaign has shown that both HSB option 1 and HSB option 2 effectively prevent stack degradation when hydrogen is not produced, no power is supplied, and the stack is kept hot. Conversely, the results of the electric protection method (HSB option 3) are unfeasible. However, the degradation of the first cells in the stack with HSB option 3 can be related to a reverse flow of air toward the stack, and additional tests should be performed to investigate the feasibility of the electric protection option without a significant flow of air toward the negative electrode.

The experimental campaign allows us to conclude that both HSB option 1 and HSB option 2 can be applied to the PROMETEO pilot plant to preserve the stack degradation when hydrogen is not produced, that is, during night hours and cloudy or rainy days, with null or limited solar irradiations. Since these two situations are quite different, it is suggested that HSB option 1 is adopted during the night and HSB option 2 otherwise. Indeed, the stack must be kept warm at night without producing hydrogen for many hours. In this case, HSB option 1, circulating an H_2-N_2 mixture through the negative electrode, limits the need for heat from the TES, which is instead used in HSB option 2 to evaporate the water, lately condensed and expelled. Conversely, HSB option 2, circulating H_2-H_2O steam mixture in the negative electrode, is suggested in case of unpredictable power unavailability, such as in case of a cloud passage lasting less than 1 h. In this case, the limited duration of the event suggests using a more straightforward solution, in which heat to vaporize the steam is justified by the lower time required to start hydrogen production again when power returns available, avoiding the time to restart the evaporator.

3.2 | Hydrogen generation control definition

The experimental campaign described in Section 2.3, by testing the SOE stack in different operating conditions, has allowed finding out how the stack temperature, the steam flow rate, and the hydrogen concentration in the steam at the cathode inlet affect the hydrogen generation.

Values of the main parameters measured during Phase 1 of the experimental campaign are shown in Figure 5. It has to be noted that since it is not possible to measure the flow rate of steam between the steam generator and the stack, its value is estimated with the water flowrate entering the steamer (green line in Figure 5a) since the two values are equal at steady state. The water flow rate entering the steamer is ramped-up and -down over time between a minimum value of about 360 g/h and a maximum value of about 1900 g/h. The hydrogen flow rate entering the system (light-blue line in Figure 5c) varies

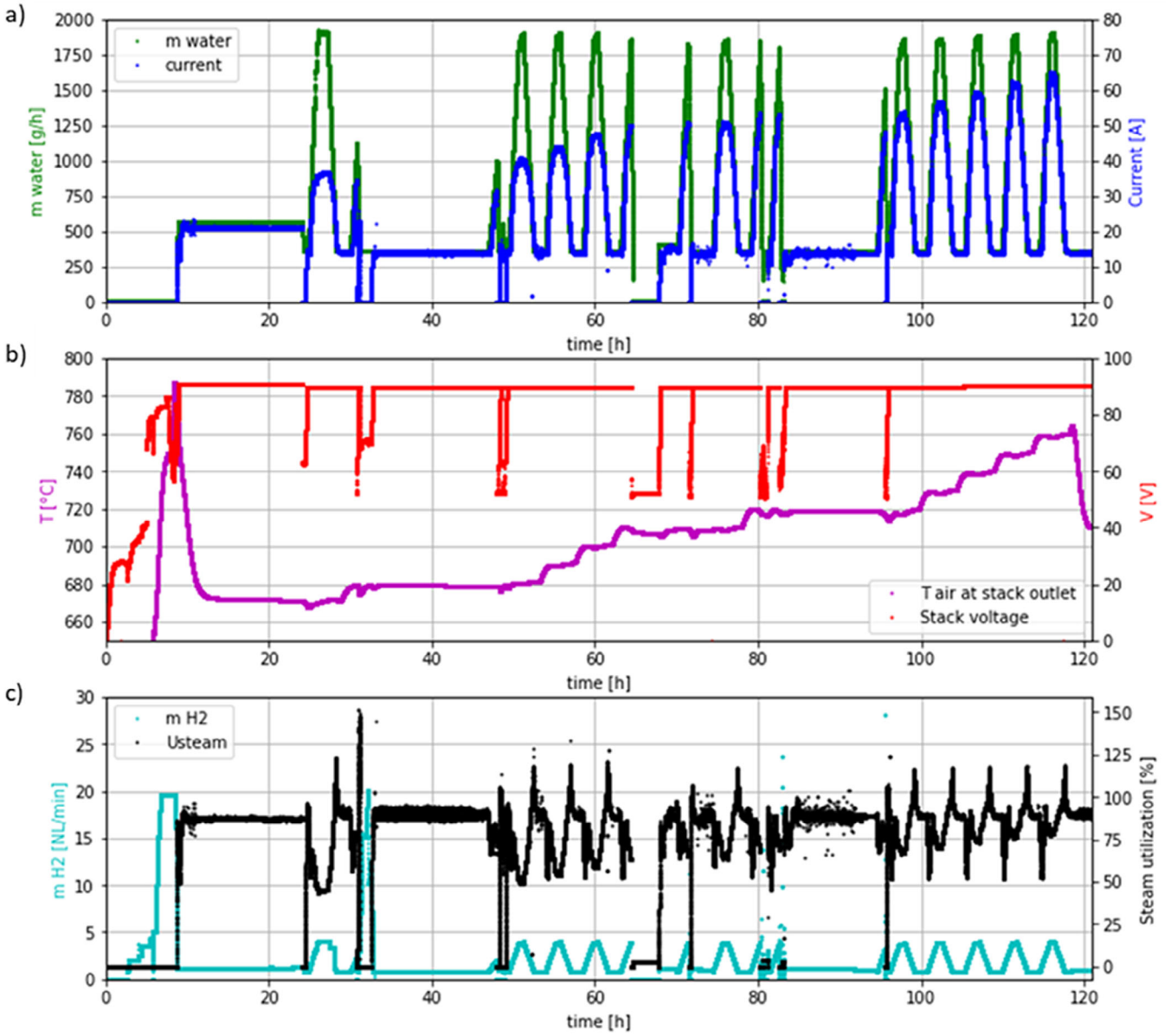

FIGURE 5 Measured data over time in test Phase 1: (a) water flowrate at system inlet, stack current, (b) stack temperature, stack voltage, (c) hydrogen flowrate at system inlet and computed steam utilization.

proportionally to the water flow rate setpoint because the control system acts to keep a 10% volume of hydrogen in the overall steam and hydrogen flow entering the stack. The system temperature setpoint is increased before each ramp-up of the water flow rate. The temperature setpoints range from 670 to 760°C, with a temperature step of 10°C. The temperature of the air at the stack outlet (magenta line in Figure 5b), which is representative of the stack temperature, has negligible oscillations related to the steam flow rate fluctuation, thanks to the action of the control system.

Additionally, it is possible to see the temperature increase during the first hours of operation, corresponding to the system preheating phase. Once the preheating phase is completed, the stack voltage is set at the thermoneutral value (90.7 V) and kept constant until the end of the test. However, some sudden drops in the stack voltage are present (vertical red line in Figure 5b). They are related to failures of test bench operation, such as high pressure within the stack or failure in the cathode heaters.

The resulting current (blue line in Figure 5a) increases when the water flow rate increases, and vice versa it decreases when the water flow rate decreases.

The resulting steam utilization factor (black line in Figure 5c) shows values above 100%, which is unfeasible. This highlights that the water flow rate at the steamer inlet is not equal to the steam flow rate at the stack inlet. The reason is possibly related to mass transport delays or delays in the control of the steamer. This highlights that a direct measure of the steam flow rate entering the stack is required to characterize the transients

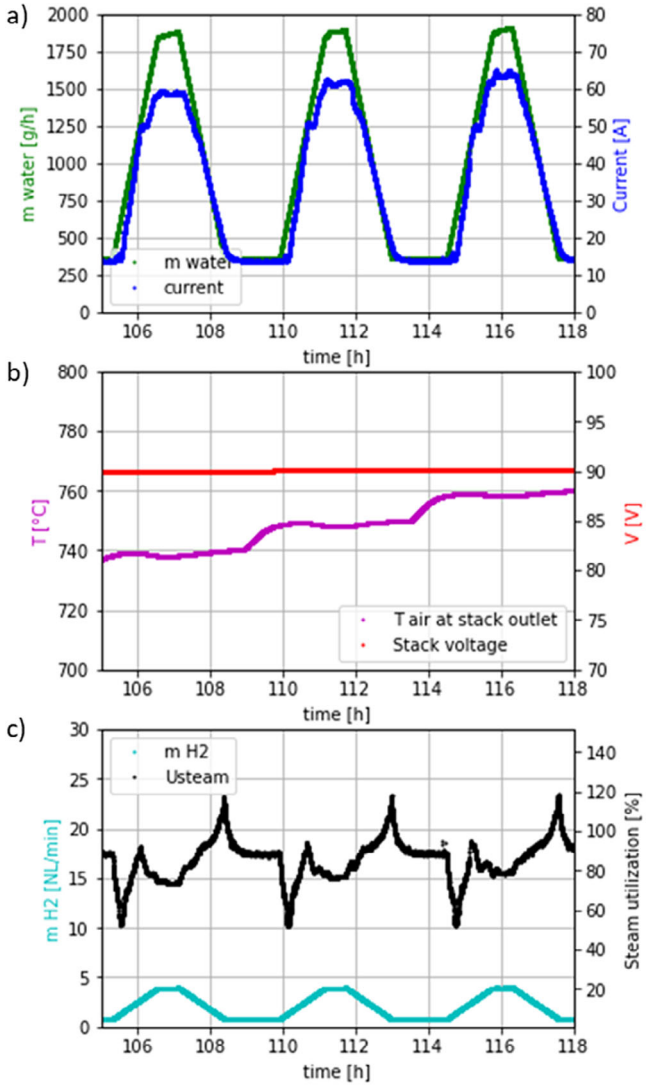

FIGURE 6 Measured data over time in test Phase 1: (a) water flowrate at system inlet, stack current, (b) stack temperature, stack voltage, (c) hydrogen flowrate at system inlet and computed steam utilization; zoom on temperature setpoints equal to 740, 750, and 760°C.

precisely. However, this improvement was not possible in the test bench used in this experimental campaign, and the following analysis is based on the water flow rate entering the evaporator.

To better investigate the effects of temperature and steam flowrate on the stack current, the values measured when the preheating phase is completed and when the stack is operated at a thermoneutral voltage (admitting an error equal to 0.2 V) have been selected. For example, Figure 6 shows the selected data over 13 h of operation, corresponding to the water ramp-up and ramp-down at 740, 750, and 760°C. The figure confirms that the water flow rate at the steamer inlet is not equal to the steam flow rate at the stack inlet. Indeed, in Figure 6a, the stack current increases only about 5–10 min after the water flow rate. The same happens during the water ramp-down, which precedes a few minutes of the current drop. For example, when the water flow rate reaches the minimum values after a ramp-down,

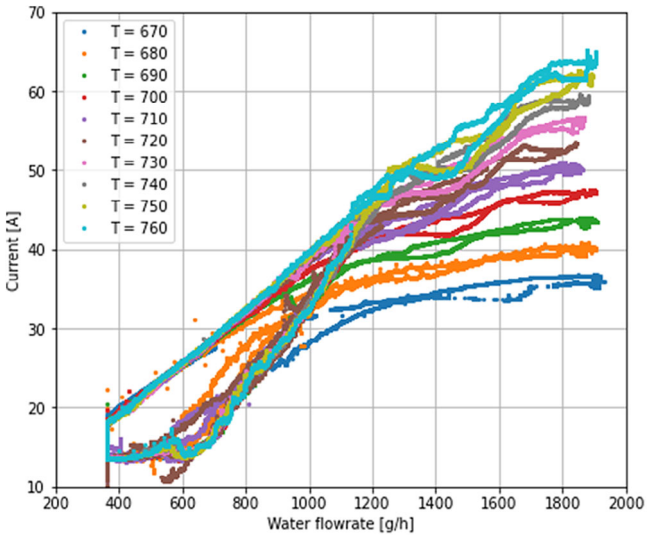

FIGURE 7 Results of experimental test Phase 1: current (A) depending on water flow rate at steamer inlet (g/h) and stack temperature (°C).

the current is not yet at the minimum, resulting in a calculated steam utilization (Figure 6c) above 100%. However, the steam flow rate at the stack inlet has not reached the minimum value, justifying the measured current value. The ability of the system to keep the temperature constant is confirmed by the negligible oscillation of the air temperature at the stack outlet (Figure 6b).

Figure 7 shows the values of the stack current as a function of the water flow rate at the steamer inlet for different stack temperatures. While a unique current value is expected for each temperature and steam flow rate value entering the stack, two points are present in Figure 7 for each water flow rate. They correspond to two different steam flow rates related to the increasing and decreasing water ramps.

While measuring the steam flowrate at the stack inlet is mandatory for a more accurate analysis, the available data are sufficient to understand that:

- With low steam flow rates, the steam flow rate limits the stack current (and therefore the hydrogen flow rate), and a variation in the stack temperature does not affect the current. These operating points correspond to the highest steam utilization factor.
- With high steam flow rates, the stack temperature limits the stack current. Increasing the steam flow rate allows working with lower steam utilization factors in these cases, but only small increases in the current are noted. Conversely, a rise in the current from about 25 A to 65 A is noted when the temperature increases from 670 to 760°C.

The minimum value of steam flow rate above which the current depends mainly on the temperature increases with the temperature itself. It is about 700 g/h at 670°C and about 1800 g/h at 760°C.

Values of the main parameters measured during Phase 2 of the experimental campaign are shown in Figure 8. The hydrogen flow rate (light-blue line in Figure 8a) entering the system,

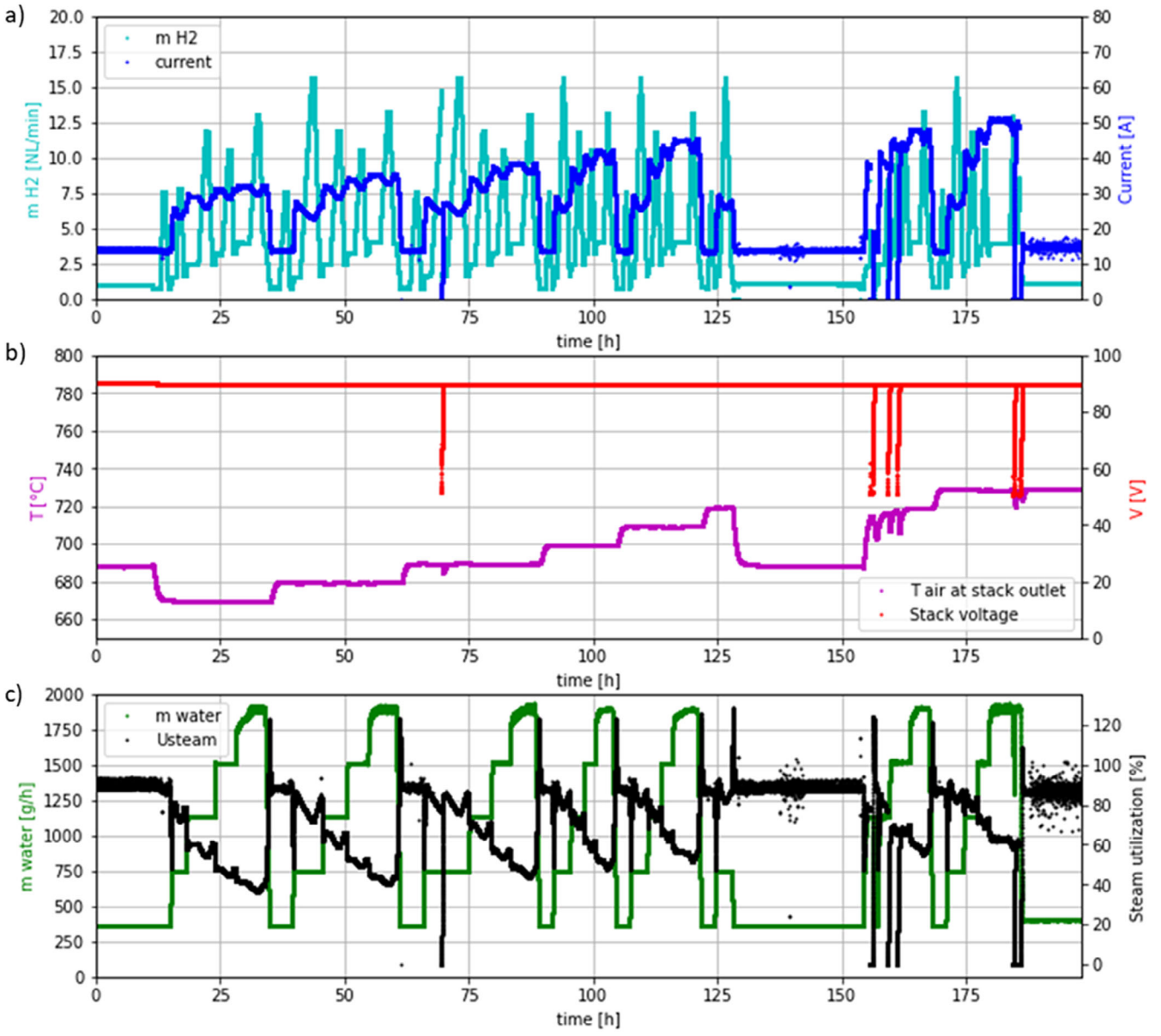

FIGURE 8 Measured data over time in test Phase 2: (a) hydrogen flow rate at system inlet, stack current, (b) stack temperature, stack voltage, (c) water flow rate at system inlet and computed steam utilization.

mixed with the steam flow before entering the electrolysis stack, is ramped-up and -down over time to vary the hydrogen fraction in the overall hydrogen and steam flow entering the stack. Each ramp-up and -down of the hydrogen flow rate corresponds to a different system temperature setpoint (magenta line in Figure 8b) and water flow rate value (green line in Figure 8c). In detail, the temperature setpoint is increased from 670 to 730°C with stepwise changes of 10°C. For each temperature setpoint, the water flow rate is increased with steps of about 400 g/h, from a minimum equal to 360 g/h to a maximum value equal to 1900 g/h. Then, it is dropped to the minimum value to repeat the test at a higher temperature. The voltage setpoint equals the thermoneutral value during the entire test, but a few deviations are recorded (red line in Figure 8b). The data measured when the voltage differs from the setpoint are discarded before performing additional data analysis.

The resulting current (blue line in Figure 8a) increases considerably when the temperature increases and when the water flow rate increases from the minimum value to the intermediate or the highest value. Conversely, the variation of the hydrogen fraction in the overall H_2-H_2O steam flow do no produce appreciable changes in the current. As an example, when the stack is at the thermoneutral voltage and the stack temperature is equal to 670°C: (i) the stack current increases by about 10 A when the water flowrate is varied from about 360 g/h to about 760 g/h and of about 5 A when it is further increased to about

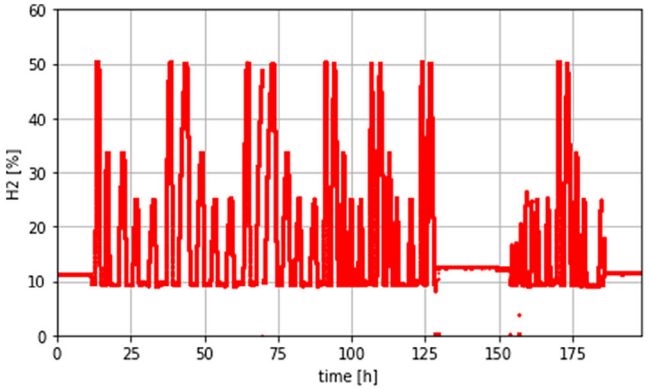

FIGURE 9 Hydrogen fraction in the overall hydrogen and steam flow over time in test Phase 2.

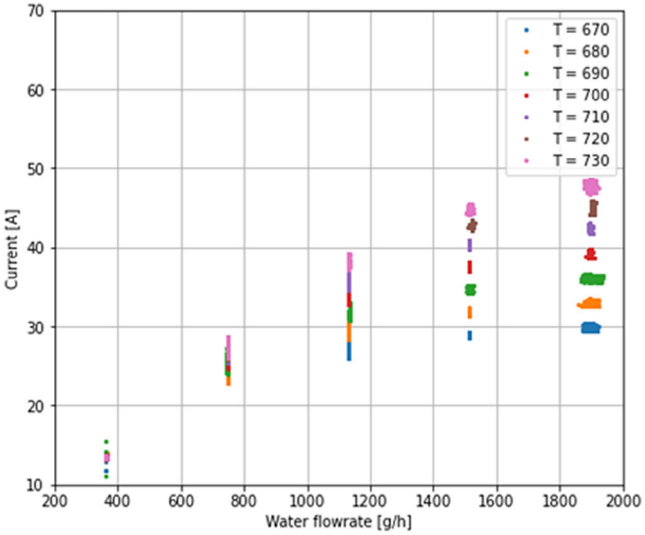

FIGURE 10 Results of experimental test Phase 2: current (A) depending on water flow rate at steamer inlet (g/h) and stack temperature (°C).

1160 g/h (low water flowrates, limiting the current), while no significant current variation are present when the water flowrate is furtherly increased (high water flowrate, current limited by the temperature); (ii) the effect of the hydrogen fraction (proportional to the hydrogen flow rate) on the current is negligible because when it increases from the minimum to the maximum value (×4 or more) the current drops of 3 A maximum (e.g. from 32 to 29 A at the highest water flowrate).

The computed steam utilization (black line in Figure 8c) decreases when the water flow rate increases. Also, in this case, steam utilization values above 100%, obtained when the water flow rate suddenly decreases, highlight that the water flow rate at the steamer inlet (used to compute the utilization factor) and the steam flowrate at the steamer outlet (determining the current) are different.

The percentage of hydrogen in the overall hydrogen and water flow is shown in Figure 9. The minimum hydrogen fraction tested is 10% since it is the minimum value required for a reducing environment. The maximum tested value is 50%. However, 50% is reached only with low water flow rates due to limits in the maximum hydrogen flow rate.

Figure 10 shows the values of the stack current as a function of the water flow rate at the steamer inlet for different stack temperatures. In this case, since the water flowrate is kept constant for a few hours between one step change and the next one, to be sure that the water flowrate at the system inlet corresponds to the steam flowrate at stack inlet, the values measured immediately after a variation of the water flowrate are discarded. The plot confirms that, at low water flow rates, the current is mainly influenced by the flow rate itself: points obtained at different temperatures overlap. Conversely, higher current corresponds to higher temperature at a high water flow rate. The spread of current values obtained at each temperature and water flow rate is due to the variation of the hydrogen fraction in the overall flow entering the stack. The lower currents correspond to a higher hydrogen fraction (the higher fraction of hydrogen prevents the steam from reaching the active sites and incrementing the Nerst voltage). Additionally, the clouds of points obtained at the highest water flow rates show the difficulty of the control system in keeping the water flow rate at the set point.

This test campaign proposes two different control strategies to control hydrogen production in the PROMETEO pilot plant. In both options, the stack is operated at the thermoneutral voltage, while the operating point (i.e. the load, identifying the current density and hydrogen generation flow rate) is defined differently. In the first proposed load control strategy, the stack works with a limited steam flow rate, reaching the maximum steam utilization. The absorbed power and the generated hydrogen flow rate vary by changing the steam flow rate supplied to the stack. In the second load control strategy, the stack works with excess steam, and the steam flow rate entering the stack does not affect the load. The absorbed power and the generated hydrogen flow rate are varied by changing the stack temperature (i.e. varying the temperature of the flows at anode and cathode inlets).

While the tests here reported have shown that both hydrogen generation control through the steam flowrates and through the temperature are effective, allowing to actually vary the hydrogen generation in a controlled manner, additional tests have to be performed in further works to compare them and assess their performance. The main performance metrics to be considered are the stack degradation and the ability in following a variable load profile generated by a renewable power plant while maximizing the overall system efficiency (including electrical and thermal consumptions).

Thus, the identified control strategies will be implemented in the PROMETEO pilot plant and tested in relevant environments. The goal is to understand which strategy allows better system integration with renewable energy sources regarding system availability and efficiency. An additional effort will be required to investigate the stack degradation associated with the two control options, evaluating their impact on the stack durability. The compatibility of the developed control strategies will be also assessed in term of compatibility with SCADA/PLC used in industries, where the cost limitation for the electronic boards leads to limited sensor sampling rate and actuator

response time, possibly impacting the successful operation of the control.

Finally, this test campaign has shown the importance of accurately control the steam flowrate. Thus, in designing the SOE system it is important to carefully design the steam generation unit and its control. Indeed, the engineering of a steam generation unit able to rapidly modulate the steam production is of paramount importance in realizing a SOE system able to efficiently work with renewable power. The use of multiple steam generators in parallel must be also evaluated when scaling-up the system for industrial applications.

4 | CONCLUSIONS

High-temperature SOE systems and renewable energy sources are efficient routes for producing green hydrogen. However, developing an effective management and control strategy is pivotal in guaranteeing a synergistic operation between the SOE system and the renewable energy sources and an effective integration with hydrogen end users.

With this in mind, the proposed work has tested a 5 kW_e SOE stack during full load, partial load and hot-standby operation and has identified how to operate the SOE system in hot standby (as required when renewable electricity in unavailable) and how to control hydrogen production according to electricity availability or hydrogen demand. The identified control methods are proposed for the 25 kWe SOE prototype built and tested within the PROMETEO Project.

A first experimental campaign allowed to compare three options to keep the system warm and prevent stack degradation when hydrogen is not produced. Good results are obtained by feeding a reducing gas at the negative electrode and air at the positive electrode without polarizing the stack. The reducing gas can be either a 20% H_2 – 80% N_2 mixture (HSB option 1) or a H_2-H_2O steam mixture (HSB option 2). Conversely, the electrical protection approach (HSB option 3), where no gas is supplied to the negative electrode and the stack is polarized to keep an average cell voltage of 1 V, generates significant stack degradation (a cluster showed 15% voltage decay in 200 h). Thus, according to the peculiarity of the standby situations, two hot standby modes are proposed for implementation and testing in the PROMETEO pilot project. An H_2-N_2 mixture is suggested overnight, to limit the prolonged use of heat from the TES to produce steam. Conversely, a H_2-H_2O steam mixture is suggested for shorter and unforeseen power unavailability, as in the case of passing clouds, to allow a faster transition to the operation mode as soon as the power is available again (longer transition times would be required to start the evaporator).

A second experimental campaign allowed to test the SOE stack at different temperatures, with different steam flow rates and different hydrogen fractions in the H_2-H_2O steam mixture supplied to the stack, to identify the impact of these parameters on hydrogen generation. All tests are performed by controlling the voltage, which is kept constant at the thermoneutral value. Voltage control allows a fail-safe control in the event of steam unavailability (no fast rise in voltage) and operation at thermoneutral voltage, although limiting the efficiency, allows to avoid temperature gradient in the cells possibly causing faster degradation. Results show that, while the amount of hydrogen in the steam entering the stack cathode does not significantly affect hydrogen production, stack temperature and steam flow rate do. According to the experimental results, two different control strategies were identified, both keeping the stack at constant voltage and differing in the way in which the hydrogen generation is controlled: (i) varying the steam flowrate supplied to the stack while working at maximum steam utilization and constant temperature, (ii) varying the stack temperature while the steam flowrate is controlled to have a low steam utilization. Both strategies result viable, allowing to control hydrogen generation, but their effectiveness and efficiency when following a variable load profile and their effect on the stack degradation must be further evaluated. Implementation of both control strategies in the 25 kW_e PROMETEO system will allows to identify pros and cons of both strategies.

Overall, in a global context, the work has shown how a high-temperature SOE stack can be fully powered by intermittent renewable energy sources, identifying methods to limit the stack degradation during hot stand-by and providing solutions to control hydrogen generation. Indeed, an effective hot standby strategy allows to prevent stack degradation whilst minimizing the heat consumption, while hydrogen generation control allows to increase the rangeability of the system, following renewable electricity generation profiles. Therefore, these solutions allow to extend the plant operation time, maximizing the plant overall efficiency.

In relation to the PROMETEO project, the work has provided valuable inputs for defining the pilot plant P&ID, identifying the sensors and controllers to be installed and the gas/mixture to be supplied in each operation mode, and providing hints on how to operate the system to guarantee a safe and effective coupling with renewable electricity and heat.

The main limitation of this work is related to the testing of the stack in laboratory environment for a limited time. Indeed, long-term testing in relevant environment is required to validate the findings and to prove the effectiveness of the proposed control strategies. Thus, next activities include the implementation of the proposed hot standby modes and control strategy options in the PROMETEO pilot plant. During plant operations, the stack performance will be monitored to proof the effectiveness of the proposed strategies in limiting the degradation. Additionally, stack and balance of plant consumptions will be monitored to assess the efficiency of the system. The realization of a simulation model of the system, validated through the pilot plant data, will allow to further optimize the system layout and operation strategy. The choice of the most efficient control strategy option will be the basis for further development of the control logic architecture of the PROMETEO plant.

NOMENCLATURE

BoP	Balance of plant
CSP	Concentrated solar panel
FBK	Fondazione Bruno Kessler

FC	Fuel cell
PV	Photovoltaic
P2G	Power to gas
P&ID	Piping and Instrumentation Diagram
SOE	Solid Oxide Electrolysis
SRU	Single Repeated Unit
TES	Thermal Energy Storage
TRL	Technology Readiness Level

AUTHOR CONTRIBUTIONS

Elena Crespi: Conceptualization; data curation; formal analysis; investigation; methodology; writing—original draft; writing—review and editing. **Francesca Panaccione**: Conceptualization; investigation; visualization; writing—original draft; writing—review and editing. **Davide Ragaglia**: Formal analysis; methodology; writing—original draft; writing—review and editing. **Matteo Testi**: Conceptualization; formal analysis; funding acquisition; project administration; resources; supervision.

ACKNOWLEDGEMENTS

The project has received funding from the Fuel Cells and Hydrogen 2 Joint Undertaking (now Clean Hydrogen Partnership) under Grant Agreement n° 101007194 - PROMETEO. The Joint Undertaking receives support from the European Union's Horizon 2020 research and innovation program, Hydrogen Europe and Hydrogen Europe Research. This paper and the research behind it would not have been possible without the support of SOLYDERA teams (Dr. Stefan Diethelm and Dr. Dario Montinaro) for the supply of the modified SOE stack and the sharing of technical specifications.

CONFLICT OF INTEREST STATEMENT

The authors declare no conflicts of interest.

DATA AVAILABILITY STATEMENT

Data available on request from the authors.

ORCID

Elena Crespi https://orcid.org/0000-0001-7388-8993

REFERENCES

1. Oshiro, K., et al.: Role of hydrogen-based energy carriers as an alternative option to reduce residuals emissions associated with mid-century decarbonization goals. Appl. Energy 313, 118803 (2022). https://doi.org/10.1016/j.apenergy.2022.118803
2. Lystbæk, N., et al.: Review of energy portfolio optimization in energy markets considering flexibility of power-to-X. Sustainability 15, 4422 (2023). https://doi.org/10.3390/su15054422
3. Colombo, P., et al.: Dynamic dispatch of solid electrolysis system for high renewable energy penetration in a microgrid. Energy Convers. Manage. 204, 112322 (2019). https://doi.org/10.1016/j.enconman.2019.112322
4. Lia, Y., et al.: Optimal distributed generation planning in active distribution networks considering integration of energy storage. Appl. Energy 210, 1073–1081 (2017). https://doi.org/10.1016/j.apenergy.2017.08.008
5. Pandiyan, A., et al.: Review on solid oxide electrolysis cell: a clean energy strategy for hydrogen generation. Nanomater. Energy 8, 2–22 (2019). https://doi.org/10.1680/jnaen.18.00009
6. Khan, F., et al.: Recent development in electrocatalysts for hydrogen production through water electrolysis. Int. J. Hydrogen Energy 46(63), 32284–32317 (2021). https://doi.org/10.1016/j.ijhydene.2021.06.191
7. Noro, M., et al.: Enhancement of energy generation efficiency in industrial facilities by SOFC e SOEC systems with additional hydrogen production. Int. J. Hydrogen Energy 44(19), 9608–9620 (2019). https://doi.org/10.1016/j.ijhydene.2018.08.145
8. AlZahrani, A.A., et al.: Thermodynamic and electrochemical analyses of a solid oxide electrolyzer for hydrogen production. Int. J. Hydrogen Energy 42(33), 21404–21413 (2017). https://doi.org/10.1016/j.ijhydene.2017.03.186
9. Barelli, L., et al.: Airflow management in solid oxide electrolyzer (SOE) operation: performance analysis. ChemEngineering 1(2), 13 (2017). https://doi.org/10.3390/chemengineering1020013
10. Ferrero, D., et al.: Reversible operation of solid oxide cells under electrolysis and fuel cell modes: Experimental study and model validation. Chem. Eng. J. 274, 143–155 (2015). https://doi.org/10.1016/j.cej.2015.03.096
11. Zhang, X., et al.: Improved durability of SOEC stacks for high temperature electrolysis. Int. J. Hydrogen Energy 38(1), 20–28 (2017). https://doi.org/10.1016/j.ijhydene.2012.09.176
12. Hauch, A., et al.: Recent advances in solid oxide cell technology for electrolysis. Science 370, eaba6118 (2020). https://doi.org/10.2172/1513461
13. Sun, Y., et al.: Solid oxide electrolysis cell under real fluctuating power supply with a focus on thermal stress analysis. Energy 261, 125096 (2022). https://doi.org/10.1016/j.energy.2022.125096
14. Min, G., et al.: A review of solid oxide steam-electrolysis cell systems: thermodynamics and thermal integration. Appl. Energy 328, 120145 (2022). https://doi.org/10.1016/j.apenergy.2022.120145
15. Giap, V.T., et al.: High efficient reversible solid oxide fuel cell coupled with waste steam for distributed electrical energy storage system. Renewable Energy 144, 129–138 (2019). https://doi.org/10.1016/j.renene.2018.10.1120
16. Rivera-Tinoco, C., et al.: Competitiveness of hydrogen production by high temperature electrolysis: impact of the heat source and identification of key parameters to achieve low production costs. Energy Convers. Manag. 51(12), 2623–2634 (2010). https://doi.org/10.1016/j.enconman.2010.05.028
17. Sigurvinsson, J., et al.: Can high temperature steam electrolysis function with geothermal heat. Int. J. Hydrogen Energy 32(9), 1174–1182 (2007). https://doi.org/10.1016/j.ijhydene.2006.11.026
18. Schiller, G., et al.: Solar heat integrated solid oxide steam electrolysis for highly efficient hydrogen production. J. Power Sources 416, 72–78 (2019). https://doi.org/10.1016/j.jpowsour.2019.01.059
19. Mottaghizadeh, P., et al.: Process modeling of a reversible solid oxide cell (r-SOC) energy storage system utilizing commercially available SOC reactor. Energy Convers. Manage. 142, 477–493 (2017). https://doi.org/10.1016/j.enconman.2017.03.010
20. Liu, H., et al.: Assessing fluctuating wind to hydrogen production via long-term testing of solid oxide electrolysis stacks. Appl. Energy 361, 122938 (2024). https://doi.org/10.1016/j.apenergy.2024.122938
21. Petipas, F., et al.: Transient operation of a solid oxide electrolysis cell. Int. J. Hydrogen Energy 38, 2957–2964 (2013). https://doi.org/10.1016/j.ijhydene.2012.12.086
22. Prometeo project website. https://prometeo-project.eu/project/. Accessed 4 Jan 2024
23. Crespi, E., et al.: Control of a solid oxide electrolysis system for hydrogen generation from solar power and thermal energy storage. In: 2023 International Conference on Clean Electrical Power (ICCEP), pp. 765–774. IEEE, Piscataway, NJ (2023)
24. Udagawa, J., Aguair, P., Brandon, N.P.: Hydrogen production through steam electrolysis: control strategies for a cathode-supported intermediate temperature solid oxide electrolysis cell. J. Power Source 180(1), 354–364 (2008). https://doi.org/10.1016/j.jpowsour.2008.01.069
25. Fragiacomo, P., et al.: Design of an SOFC/SOE station: planning of simulation tests. Energy Proc. 148, 535–542 (2018). https://doi.org/10.1016/j.egypro.2018.08.137

26. Fragiacomo, P., et al.: Design of an SOFC/SOE station: experimental test campaigns. Energy Proc. 148, 543–550 (2018). https://doi.org/10.1016/j.egypro.2018.08.005
27. Barelli, L., et al.: Air variation in SOE: stack experimental study. Int. J. Hydrogen Energy 43, 11655–11662 (2018). https://doi.org/10.1016/j.ijhydene.2018.01.070
28. Peters, R., et al.: Long-term experience with a 5/15 kW-class reversible solid oxide cell system. J. Electrochem. Soc. 168, 014508 (2021). https://doi.org/10.1149/1945-7111/abdc79
29. Lu, B., Zhang, Z., Zhang, Z., Zhang, C., Zhu, L., Huang, Z.: Control strategy of solid oxide electrolysis cell operating temperature under real fluctuating renewable power. Energy Convers. Manage. 299, 117852 (2024). https://doi.org/10.1016/j.enconman.2023.117852
30. Cai, Q., Adjiman, C.S., Brandon, N.P.: Optimal control strategies for hydrogen production when coupling solid oxide electrolysers with intermittent renewable energies. J. Power Sources 268, 212–224 (2014). https://doi.org/10.1016/j.jpowsour.2014.06.028
31. Botta, G., Romeo, M., Fernandes, A., Trabucchi, S., Aravind, P.V.: Dynamic modeling of reversible solid oxide cell stack and control strategy development. Energy Convers. Manage. 185, 636–653 (2019). https://doi.org/10.1016/j.enconman.2019.01.082
32. EBZ gmbh. https://www.ebz-dresden.de/. Accessed 24th Oct 2024
33. SolydEra. https://solydera.com/it/. Accessed 24th Oct 2024
34. Faes, A., et al.: A review of RedOx cycling of solid oxide fuel cells anode. Membranes 2, 585–664 (2012)
35. Kim, Y.J., et al.: Thermal cycling of anode supported solid oxide fuel cells under various conditions: electrical anode protection. Int. J. Hydrogen Energy 41, 23173–23182 (2016)

How to cite this article: Crespi, E., Panaccione, F., Ragaglia, D., Testi, M.: Integration of a solid oxide electrolysis system with solar thermal and electrical energy: A testing campaign for operation and control strategy definition. IET Renew. Power Gener. 1–15 (2024). https://doi.org/10.1049/rpg2.13141